

Electronic Supplementary Information (ESI)

Variable structural colouration of composite interphase

*Yinhu Deng,^{ab} Shanglin Gao,^{*a} Jianwen Liu,^a Uwe Gohs,^a Edith Mäder^{ab} and Gert Heinrich^{ab}*

^a Department of Composite Materials, Leibniz-Institut für Polymerforschung Dresden e. V. (IPF), Hohe Strasse 6, Dresden 01069, Germany . Email: gao@ipfdd.de

^b Faculty of Mechanical Science and Engineering, Technische Universität Dresden (TU Dresden), George-Bähr-Strasse 3c, Dresden 01069, Germany

Experimental methods

Alkali-resistant glass fibres (ARG) with an average diameter of 22 μm manufactured at Leibniz-Institut für Polymerforschung Dresden e. V. by a continuous spinning process. We generated GNPs based on a modified liquid-phase exfoliation graphite method to avoid the inferior effect to electrical conductivity from conventional graphite oxide reduction method. Mixtures of 0.5 g graphite particles and 0.6 g SDBS surfactant are dissolved in 50 g Millipore water. Adding a surfactant to a solvent prior to sonication prevents restacking by adsorbing to the graphene's surface. A stable diffusion of GNPs in aqueous solution was in turn achieved through the bath sonication (up to 30 hours) and centrifugation process (4000 rpm for 40 minutes). To achieve overlapped parallel multilayer structures and electrically conducting networks of carbon nanoparticles (GNPs) on the glass fibre surface, a layer-by-layer self-assembly approach was developed (ESI,† Fig. S3). The glass fibres were placed on a glass slide with separated distance of a few tens of micrometers, and then a droplet GNP solution was dropped onto the glass slide and the imbedded fibres in the solution were coated with GNPs as water evaporated until the solution was dried at 60 °C. As the water evaporates, layer-by-layer self-assembles onto the glass fibre and in turn forms multilayer structures. The coated fibres were washed with Millipore water. Because of the capillary flow mainly on the lower surface of the glass fibre, which faces to the glass slide, the carbon nanoparticles are not equally distributed onto the whole fibre surface by a single step coating process. Then, we repeat the coating and washing process for about 5-10 times, so that relative uniform surfaces with homogeneous and continuous distribution of GNPs are obtained, which suppresses the “coffee ring” effect occurring in a conventional dip coating process. Finally, the fibres were dried in a vacuum oven at 60 °C for 8 hours and stored under standardized air-condition ($RH = 50\%$, $T = 23\text{ °C}$) for 15 days before the tests. In this work, GNPs exhibit an anisotropic shape with a large diameter/thickness aspect ratio (ESI,† Fig. S2), which provide support for the view that the anisotropic shape of the particles can deform air–water interface, producing interparticle capillary interactions and leading to the elimination of the “coffee ring” effect.⁵¹ The deposition process has always been highly reproducible and more than a few hundred single fibers were well coated. It is worth to note that the conventional dip coating method with typical immersing in and drawing out of the fibre produced a inhomogeneous GNP distribution with a no-uniform island-like structure on the fibre surface because of discontinuity by the Rayleigh instability, causing a discontinuous electrical path (electrical insulation) along the fibre direction.

For fabricating a single fibre/epoxy composite, a single fibre was mounted within a dog-bone shaped mould. A commercial DGEBA-based epoxy resin and curing agent (Hexion Specialty Chemicals Stuttgart GmbH) were thoroughly mixed and degassed as polymer matrix prior to pouring into the mould. The samples were isothermally cured at 80 °C for 12 h and then slowly cooled down to room temperature with two types of dimensions. Dimensions of 0.3 mm in thickness, 1.5 mm in width and 10 mm in gauge length of the dog bone shaped specimens are prepared for electrical resistance test and those of 1 mm in thickness, 2 mm in width and 25 mm in gauge length are prepared for observing interphase optical phenomena.

For characterisation of overlapped parallel multilayer GNPs on fibre surfaces and composite interphases, the surface morphologies were studied using atomic force microscopy (AFM, a Digital Instruments D3100, USA), transmission electron microscope (TEM Zeiss Libra200, Germany), and scanning electron microscope (FE–SEM Ultra 55, Carl Zeiss SMT AG, Germany). Image mean roughness was calculated from about AFM images of fibre surfaces, which is arithmetic average of the absolute values of the surface height deviations within the eighty cursor boxes ($1 \times 1 \mu\text{m}^2$). The structure colouration from multiple reflections of the single fibre surface and fibre/epoxy composite interphases was photographed using optical microscope equipped with KEYENCE RZ lens and a broadband LED light lamp as the illumination source (VH–1000, Keyence Corporation, Japan). The electrical resistance of the single fibre and the single fibre/epoxy composite under tensile load was monitored simultaneously with mechanical stress-strain behaviour. The stress-strain curve was detected by FAVIGRAPH Semiautomatic Equipment (Textechno Company, Germany) with a test velocity at 0.2 mm/min. A Keithley 2001 multimeter with constant test current (10 μA /700 nA) was used for electrical resistance measurements; the ends of the samples and test grips were painted with silver paste in order to form an ohmic contact.

Reference

S1 P. J. Yunker, T. Still, M. A. Lohr and A. G. Yodh, *Nature*, 2011, **476**, 308–311.

Analyses for compressing stress on fibre surface

Consider a single continuous fibre embedded in matrix, and suppose the whole composite is stretched by an axial strain.

The relationship of compressing stress and tensile strain is given as below:³⁵

$$\sigma_i = \frac{2\varepsilon_c(v_m - v_f)V_m}{\left[\frac{V_m}{k_f} + \frac{V_f}{k_m} + \frac{1}{G_m} \right]} \quad (S1)$$

where σ_i is the compressing stress onto fibre surface that is normal to the fibre surface of circular symmetry, ε_c is axial strain, v is Poisson's ratio, V is the volume fraction, k is the plane strain bulk modulus and G the shear modulus. The subscripts f and m refer to fibre and matrix.

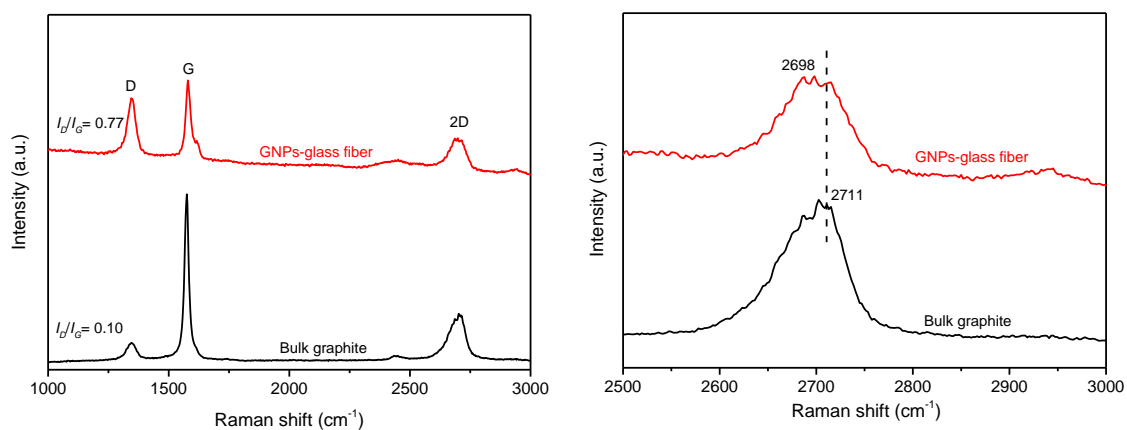


Fig. S1 Raman spectra of GNPs and pristine graphite. Raman spectra for GNPs deposited on a glass fibre and pristine graphite in the presence of disorder in the focal spot of the laser with excitation wavelength of 532 nm. Three bands are of note: the D band ($\approx 1350\text{ cm}^{-1}$), the G band ($\approx 1600\text{ cm}^{-1}$), and the 2D band ($\approx 2700\text{ cm}^{-1}$). A broad 2D band indicates that GNPs mainly with multilayers (> 5 layers). The D band gives evidence of the presence of defects, that is, either edges or topological defects in the sheet. The D-to-G band intensity ratio, I_D/I_G , is used to quantify the defect level, which increases after the intensive sonication and deposition processes from 0.1 for the pristine graphite to 0.77 for the GNPs. The intensity ratio of GNPs is consistent with the typical values (0.35~1.4) reported in the literature, generally below those of r-GO, which indicates that the concentration of defects is relatively low in the coated GNPs. A quite sharp shape of the G peak is consistently observed, suggesting a low concentration of defects since higher disorder in graphite material would lead to a much broader G peak.

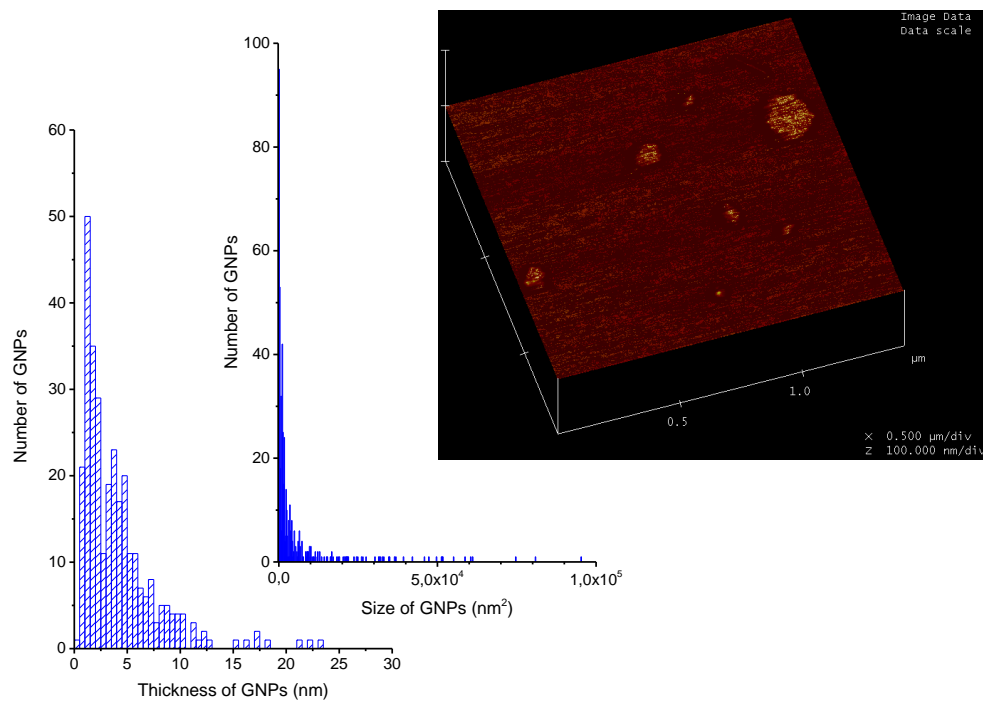


Fig. S2 Statistical analysis of thickness and size of GNPs. AFM image of individual GNPs on mica. Histograms show the distributions of the grain size and thickness of individual GNPs determined from AFM images. Statistical analyses show that the size values of GNPs are distributed widely but mostly below $1 \times 10^4 \text{ nm}^2$. The square mean root grain size and thickness are $2.1 \times 10^4 \text{ nm}$ and 5.4 nm^2 , respectively. The thickness values follow an approximately log-normal distribution and are mainly distributed between 1 and 5 nm (in terms of layers: 2 ~ 10 layers) in good agreement with the Raman spectroscopy results.

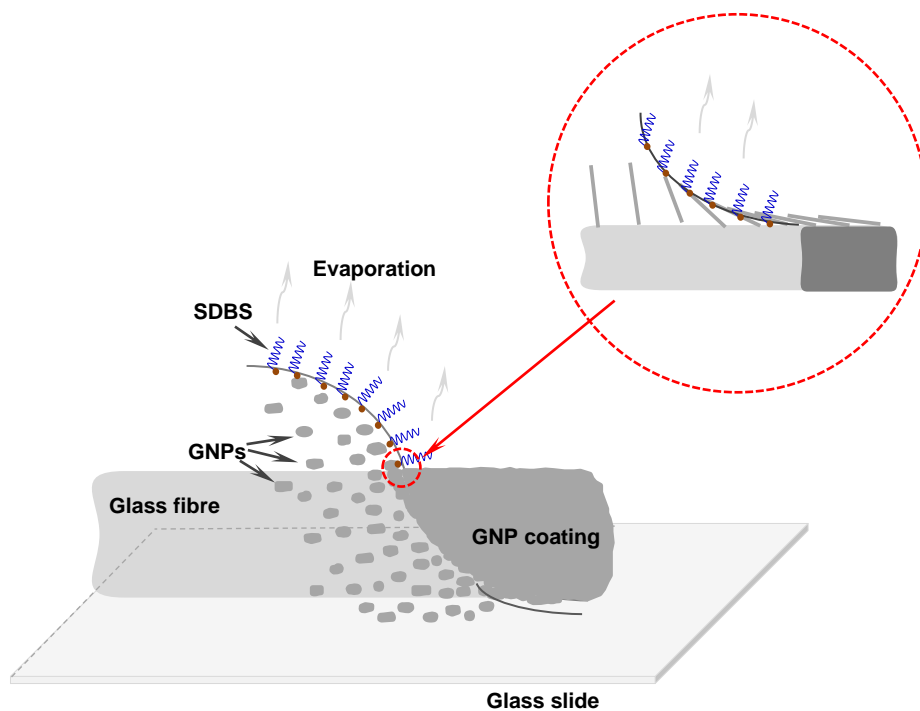


Fig. S3 Deposition process of GNPs at ambient conditions. Schematic for the deposition process of GNPs onto a single glass fibre surface based on fibre oriented capillary flow method. The overlapping multilayer structure is formed by a layer-by-layer self-assembly process, that involves standing GNPs one by one in long lines along the fibre surface so that when the first multilayer GNP plate is toppled by the moving water-air front, it topples the second, which topples the third, etc., resulting in all of the plates overlapping, which is similar to the Domino show.

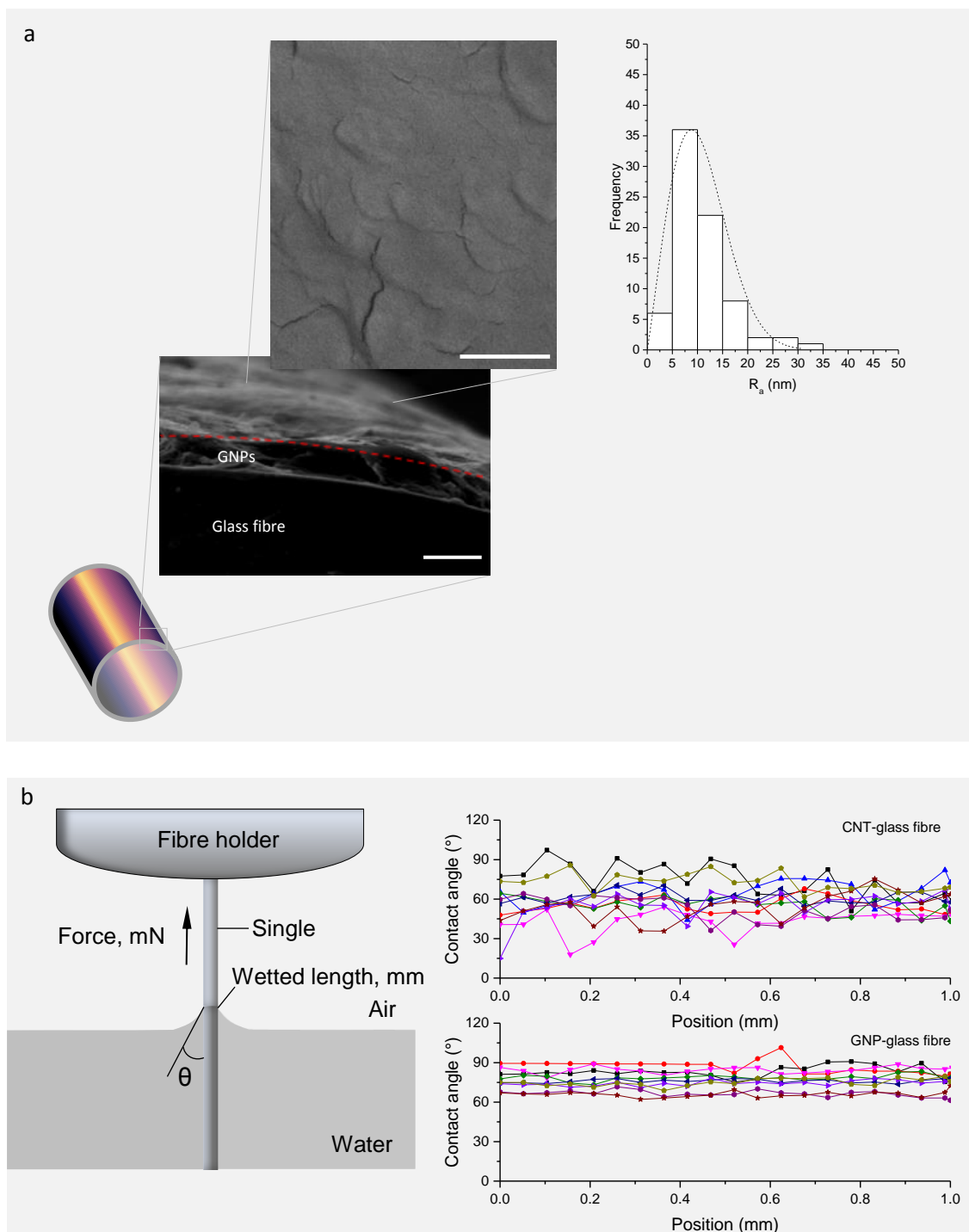


Fig. S4 Multilayer GNPs on glass fibre surface. (a) Schematic illustration of a single GNPs-glass fibre and SEM images showing overlapping surface structure and a cross-sectional view of GNP deposition on fibre surface with thickness at nano/submicron scale. Histogram of the surface roughness (mean \pm standard deviation, $R_a = 10.6 \pm 5.5$ nm) together with Weibull distribution analysis (black dash curve) characterised by AFM. Scale bars: 1 μm . (b) Surface topography variation examined using water contact angle measurements. Schematic of experimental setup of surface contact angle test for a

single fibre. The variation of dynamic advancing contact angles versus immersion depth for a single GNP-glass fibre and a single CNT-glass fibre in water. Nine specimens were tested. Since contact angle data often scatter significantly, such fluctuations are usually caused by surface roughness. The smaller data scattering of contact angle of GNP-glass fibre with water suggests overall uniform overlapping deposition of GNP layers with an ordered arrangement of nanostructure on the whole fibre surface.

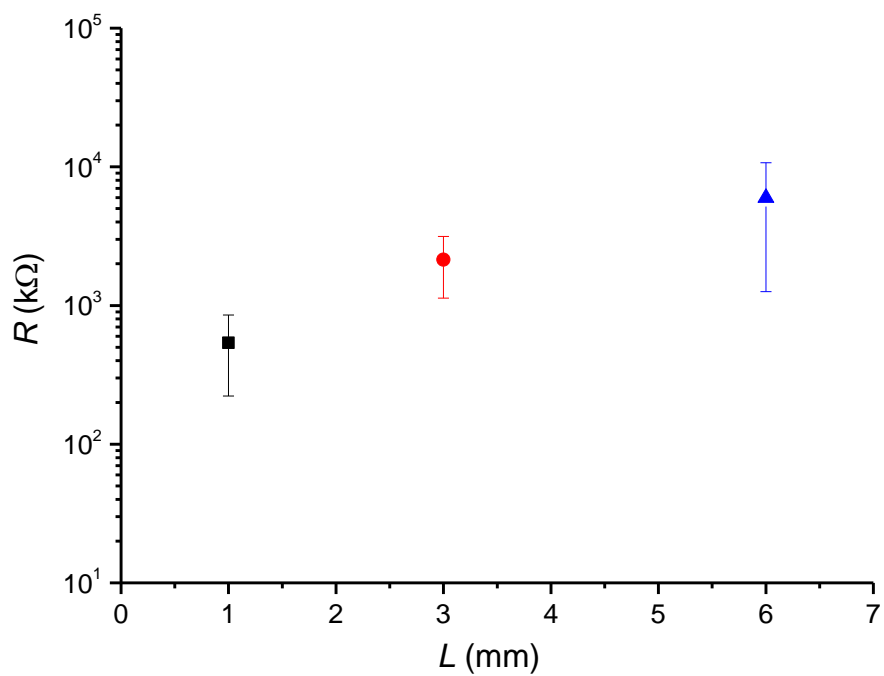


Fig. S5 Characterisation of DC electrical resistance for a single GNPs-glass fibre. The resistance R versus the distance L between electrodes, showing that the resistance increases with increasing electrode-electrode distance L , and the resistance R of a single GNPs-glass fibre within a range of 10^5 up to $10^7 \Omega$.

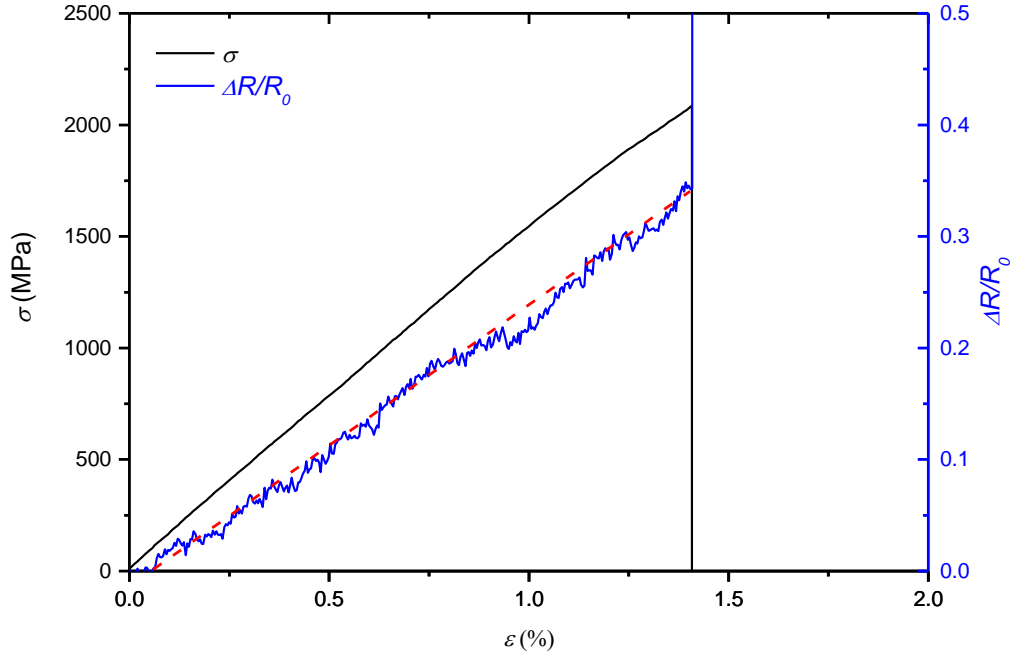
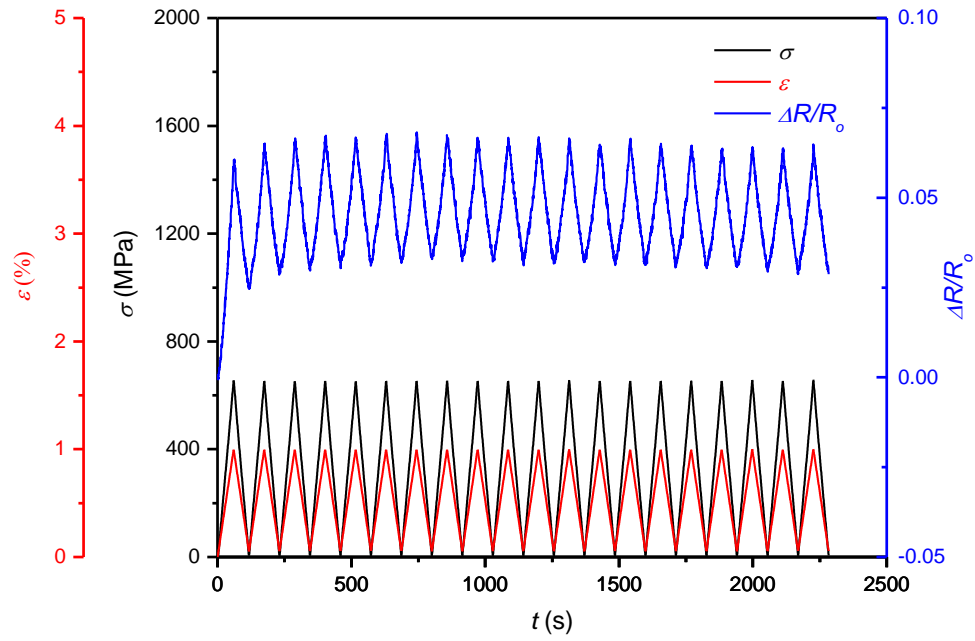


Fig. S6 Piezoresistive behaviour of a single GNPs-glass fibre. The relative resistance changes $\Delta R/R_0$ and linear regression (dotted line) of a single GNPs-glass fibre during static tensile stress up to fracture. $\Delta R/R_0$ increases approximately linearly with tensile strain, which can also be empirically described as:

$$\varepsilon = \frac{1}{GF} \frac{\Delta R}{R_0} + \varepsilon_0 \quad (S2)$$

where R_0 is the initial resistance of the specimen without applying stress, $\Delta R = R - R_0$ is the resistance change, and the parameter ε_0 , refers to the initial strain for piezoresistive effect of GNP coating, GF is the strain sensitivity factor (or known as gauge factor). Notably, the GF of our GNPs-glass fibre is more than 25, showing much more sensitive to mechanical deformation than most commercial strain sensors with GF of 2.0-3.2. The onset strain $\varepsilon_0 < 0.1\%$ for recognizing the smallest mechanical deformation with piezoresistive effect is extremely low in comparison with literature data and our previous work based on CNTs, so that the single GNPs-glass fibre has higher sensitivity even under small strain level.

a



b

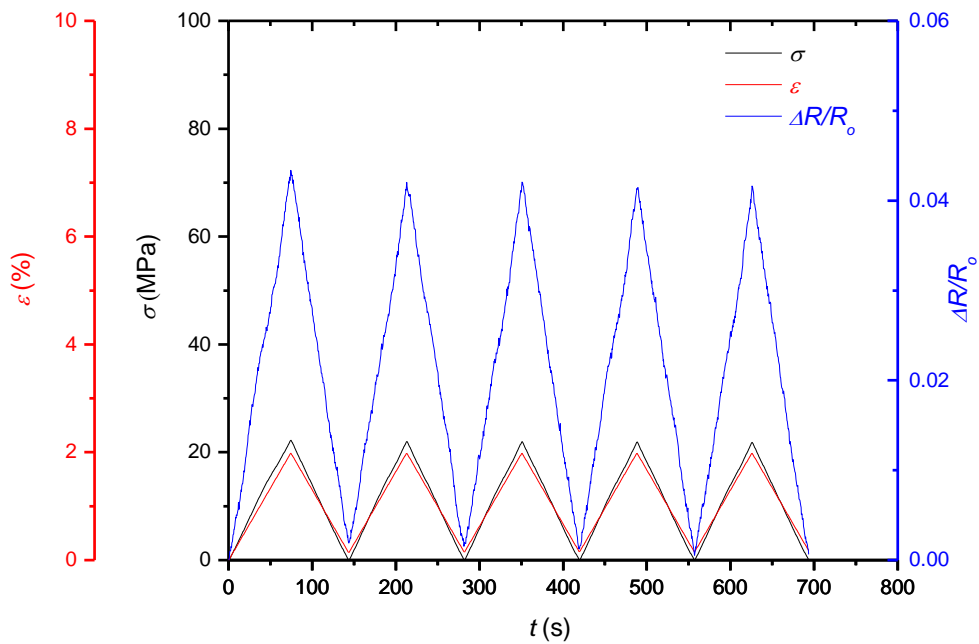


Fig. S7 Piezoresistive behaviour of a single GNPs-glass fibre (a) before and (b) after imbedded in epoxy matrix subjected to cyclic tensile loading. The electrical resistance showing good overall reversibility and repeatability response to cyclic tensile loading in “safety” strain range, corresponding to the structural colour of Orange.